Developmental Biology **243,** 81–98 (2002)

Bmp Activity Gradient Regulates Convergent Extension during Zebrafish Gastrulation

Dina C. Myers,[1] Diane S. Sepich,[1] and Lilianna Solnica-Krezel[2]

Department of Biological Sciences, Vanderbilt University, VU Station B 351634, Nashville, Tennessee 37235-1634

During vertebrate gastrulation, a ventral to dorsal gradient of bone morphogenetic protein (Bmp) activity establishes cell fates. Concomitantly, convergent extension movements narrow germ layers mediolaterally while lengthening them anteroposteriorly. Here, by measuring movements of cell populations *in vivo,* we reveal the presence of three domains of convergent extension movements in zebrafish gastrula. Ventrally, convergence and extension movements are absent. Lateral cell populations converge and extend at increasing speed until they reach the dorsal domain where convergence speed slows but extension remains strong. Using dorsalized and ventralized mutants, we demonstrate that these domains are specified by the Bmp activity gradient. *In vivo* cell morphology and behavior analyses indicated that low levels of Bmp activity might promote extension with little convergence by allowing mediolateral cell elongation and dorsally biased intercalation. Further, single cell movement analyses revealed that the high ventral levels of Bmp activity promote epibolic migration of cells into the tailbud, increasing tail formation at the expense of head and trunk. We show that high Bmp activity limits convergence and extension by negatively regulating expression of the *wnt11* (*silberblick*) and *wnt5a* (*pipetail*) genes, which are required for convergent extension but not cell fate specification. Therefore, during vertebrate gastrulation, a single gradient of Bmp activity, which specifies cell fates, also regulates the morphogenetic process of convergent extension.

Key Words: **convergence; extension; morphology; dorsoventral patterning; morphogenesis.**

INTRODUCTION

The vertebrate body plan is established by precisely coordinated inductive and morphogenetic processes of gastrulation (Schoenwolf and Smith, 2000). Mesendodermal cells migrate beneath ectoderm, creating the germ layers, which spread in the process of epiboly. Concurrent convergent extension (CE) movements that lead to mediolateral narrowing (convergence) and anteroposterior lengthening (extension) of tissue define the embryonic axis (Keller and Danilchik, 1988; Schoenwolf and Smith, 2000). It has been suggested that gastrulation movements may be regionalized (Kane and Warga, 1994), but these "domains of movement" have not been characterized. Concomitant with gastrulation movements, cell fates are being specified. A large body of evidence indicates that cell fates in the vertebrate gastrula are specified chiefly by a ventral to dorsal bone morphogenetic protein (Bmp) activity gradient, established partly by the secretion of Bmp antagonists from the dorsal gastrula organizer (Jones and Smith, 1998; Piccolo *et al.*, 1996, 1999). In contrast, the genetic mechanisms that regulate CE movements and coordinate them with cell fate specification events are less well understood (Peifer and Polakis, 1999; Solnica-Krezel, 1999).

The morphogenetic process of CE has been best characterized in *Xenopus,* where mesenchymal cells move as a sheet, driving both convergence and extension (Keller *et al.*, 2000). The main CE cell behavior is mediolateral cell intercalation driven by bipolar or unipolar protrusive activity (Keller *et al.*, 1991, 1992). In *Xenopus,* CE contributes significantly to involution and epiboly, as CE defects impair both of these processes (Shih and Keller, 1994).

CE movements in teleosts exhibit both similarities and striking contrasts to those in *Xenopus.* Whereas ectodermal cells form a sheet similar to the frog gastrula, mesodermal cells migrate as individuals or groups (Concha and Adams, 1998; Trinkaus *et al.*, 1992). Furthermore, in teleosts convergence and extension movements are not always linked.

[1] D.C.M. and D.S.S. contributed equally to this work.
[2] To whom correspondence should be addressed. Fax: 615-343-6707. E-mail: lilianna.solnica-krezel@vanderbilt.edu.

0012-1606/02 $35.00

Lateral mesodermal cells of *Fundulus* gastrulae migrate dorsally contributing to convergence and thickening of tissue, rather than its extension (Trinkaus *et al.*, 1992). Convergence and extension movements in teleosts may result from a combination of cell behaviors. Dorsal cells elongate, align mediolaterally and engage in intercalation (Topczewski *et al.*, 2001; Concha and Adams, 1998; Warga and Kimmel, 1990), whereas lateral cells migrate dorsalward predominantly by filolamellipodia, with little intercalation (Trinkaus *et al.*, 1992). In another contrast to *Xenopus*, zebrafish mutations that impair CE movements do not significantly affect involution or epiboly (Solnica-Krezel, 1999; Sepich *et al.*, 2000; Heisenberg *et al.*, 2000).

Recent studies indicate that Wnt signaling is essential for cell polarization underlying intercalations during CE in both frog and zebrafish. Overexpression of Wnt5a inhibits CE in *Xenopus* explants (Moon, 1993; Torres *et al.*, 1996). Zebrafish embryos with mutations in *wnt11/silberblick* (*slb*) or *wnt5a/pipetail* (*ppt*) genes have shortened embryonic axes and impaired extension (Heisenberg *et al.*, 2000; Rauch *et al.*, 1997). Similarly, *knypek* mutation, which inactivates a heparan sulfate proteoglycan of the glypican family that promotes Wnt11 signaling, impairs mediolateral cell elongation and, consequently, CE movements (Topczewski *et al.*, 2001). Furthermore, Dishevelled (Dsh) function is required in CE of *Xenopus* explants for bipolar protrusive activity and mediolateral alignment of cells (Wallingford *et al.*, 2000). Intriguingly, Wnt signaling mediating CE movements does not involve β-catenin, but rather follows a noncanonical pathway reminiscent of *Drosophila* planar cell polarity (PCP) signaling (Heisenberg *et al.*, 2000; Tada and Smith, 2000; Djiane *et al.*, 2000; Wallingford *et al.*, 2000).

Bmp signaling also has been implicated in the regulation of CE. Bmp overexpression blocks Activin-induced CE of frog animal cap explants (Jones *et al.*, 1992), whereas Bmp inhibition can instigate CE of ventral marginal zone explants (Graff *et al.*, 1994). However, in teleosts, the relationship between convergence and extension movements and Bmp signaling might be more complex. Ventral cells, which normally experience high Bmp activity, migrate vegetally (Kanki and Ho, 1997; Trinkaus, 1998). As converging lateral cell populations move dorsally toward lower Bmp levels, their speed increases; however, the rate of dorsal migration decreases again when they reach the lowest levels of Bmp activity near the dorsal midline (Sepich *et al.*, 2000; Trinkaus *et al.*, 1992). Indeed, in the dorsalized *swirl*^{tc300} (*swr, bmp2b*) mutant with decreased Bmp activity, cells accumulate ventrolaterally, suggesting defective convergence (Mullins *et al.*, 1996). These observations support the notion that convergence and extension movements may be distinct within different regions of the zebrafish gastrula and that a Bmp activity gradient may have an instructive role in establishing these CE movement domains.

To test these hypotheses, we analyzed speed and magnitude of CE movements by labeling cell populations at specific locations along the dorsoventral axis of wild-type (WT) gastrulae and measuring their dorsal translocation (convergence) or array elongation (extension). Furthermore, we analyzed convergence and extension of tissues by morphometric analyses of live embryos. These studies revealed three distinct convergence and extension domains: dorsal domain of strong extension and limited convergence, lateral domain of increasing convergence and extension movements, and ventral domain in which both convergence and extension movements are absent. Next, we uncovered an instructive role of the Bmp activity gradient in the formation of these morphogenetic domains by analyzing how convergence and extension movements of tissues, cell populations, and individual cells are altered in dorsalized and ventralized mutants (Hammerschmidt *et al.*, 1996; Schulte-Merker *et al.*, 1997). We propose a model wherein high Bmp activity levels can cell-autonomously specify a ventral region characterized by inhibited convergence and extension movements but strong vegetalward migration of the mesoderm. In lateral regions, decreasing Bmp activity specifies a region of increasing convergence and extension. Dorsally, low Bmp activity levels specify liberal extension with limited convergence by promoting mediolaterally polarized cell morphology underlying intercalation movements. In addition, we show that Bmp signaling negatively regulates *wnt11/slb* and *wnt5a/ppt* gene expression, thereby potentially limiting CE movements. Therefore, a single gradient of Bmp signaling regulates cell fate specification and convergent extension during vertebrate gastrulation.

MATERIALS AND METHODS

Fish Maintenance, Strains, and Genetic Analysis

Fish were maintained as described (Solnica-Krezel *et al.*, 1994). Homozygous mutant embryos were obtained by natural matings of heterozygous carriers for *chordino*^{tt250} (Schulte-Merker *et al.*, 1997), *somitabun*^{tc24} (Mullins *et al.*, 1996), or *bozozok chordino* (*boz*^{m168} *din*^{tt250}; Gonzalez *et al.*, 2000). *chordino*^{tt250}, through a point mutation in a donor splice site, eliminates production of the Bmp antagonist Chordin, resulting in ventralization of the embryo (Schulte-Merker *et al.*, 1997). *somitabun*^{tc24} is a dominant maternal and zygotic antimorph of Smad5, the Bmp-specific receptor Smad, thereby blocking signaling (Hild *et al.*, 1999). *boz*^{m168} produces a truncated protein lacking the homeodomain and has a very reduced ability to induce a functional organizer (Fekany *et al.*, 1999; Koos and Ho, 1998).

Morphometric Analysis of Live Embryos

Labeling of live embryos, image acquisition, and morphometric analyses were performed essentially as described previously (Sepich *et al.*, 2000). Extension of the head rudiment around the yolk was determined by measuring the dimension from the anterior tip of the head to the level of the first visible somite boundary. Statistical significance ($P \leq .05$) in all experiments was determined by the Student's *t* test using Microsoft Excel software.

Injection and Uncaging of Fluorescein for Cell Fate and Movement Analyses

Injection and uncaging of fluorescein in cell groups was performed as described by Sepich *et al.* (2000), yielding an initial label size of 80 ± 3 μm in diameter. Animal–vegetal elongation of labeled cell groups as an assay for extension was measured as described (Sepich *et al.*, 2000).

Injection of PKH2-GL and Analysis of Dorsal Migration

Injection of the lipophilic dye PKH2-GL and dorsal migration of labeled cell groups were assayed according to Sepich *et al.* (2000). As an assay for convergence movements, we measured dorsal translocation of labeled cell groups by determining an angle between the position of the labeled cell group and the dorsal midline in the course of gastrulation (Figs. 1E and 1G). To make the measurement, embryos were positioned animal or vegetal pole up and observed focusing on the equator of the embryo (Fig. 1G) with an eyepiece protractor reticule centered in the middle of the embryo. The angle between the line bisecting the labeled cell group and the line bisecting the dorsal midline was then measured. Cells were scored as migrating dorsally only if they moved from their initial location and separated from the overlying labeled enveloping layer cells.

No Convergence No Extension Zone Boundary Analysis

Groups of ventral marginal cells in WT, *sbn*, and *din* embryos were labeled by either PKH2-GL or activation of caged fluorescein. Their position relative to the dorsal midline was assayed by using an eyepiece protractor reticule as described above. In the case of *boz din* mutants, where no morphologically distinct dorsal midline forms during gastrulation (Gonzalez *et al.*, 2000), at least two marginal cell groups were randomly labeled. Convergence of the labeled populations was analyzed at the end of the gastrula period by assessing whether the labeled cells moved laterally from their initial location. *boz din* mutants were fixed at this time and further analyzed by *in situ* hybridization for *papc* expression and antibody staining to reveal the position of the labeled cells. The anteroposterior extension of the labeled cell array was analyzed by assessing its animalward elongation beyond the vegetal *papc* expression domain.

In Situ Hybridization and Fate Mapping

In situ hybridization and fate mapping analyses were performed as described (Sepich *et al.*, 2000). Processed embryos were mounted in 100% glycerol and photographed by using a Zeiss Axiophot microscope and an Axiocam digital camera or 35-mm camera.

Transplantation

Donor embryos were first injected with synthetic RNA encoding constitutively active Bmp type I receptor (Nikaido *et al.*, 1999) at the one-cell stage followed by a mixture of 3% rhodamine and 3% biotin dextran (Molecular Probes). Cells from the margin of donor embryos were transplanted to the margin of wild-type hosts 4–5 h postfertilization (hpf). The position of transplanted cells relative to dorsal was determined as described above at 6 hpf, followed by observation of the anteroposterior position at 9.5–10 hpf. Embryos were fixed with 4% paraformaldehyde and analyzed by whole-mount *in situ* hybridization for *six3* and *papc* expression. Transplanted cells were visualized by HRP–strepavidin and DAB substrate staining.

Confocal Image Collection and Cell-Shape Analyses

Embryos with widely scattered labeled cells were generated by injecting a bead of DiI in soybean oil (Wesson) into 1 cell of an 8- to 32-cell-stage embryo (Cooper *et al.*, 1999). Between yolk plug closure and the two-somite stage, Z-series images were collected at 3-μm intervals, using a Zeiss LSM 410 Confocal Laser Scanning Inverted Microscope (at the Vanderbilt University Medical Center Cell Imaging Core Resource, supported by NIH Grants CA68485 and DK20593). Dimensions and orientation of cells were determined by using NIH Image 1.62. Aspect ratios were calculated by using Microsoft Excel. Watson's U^2 tests for significance and Rose Diagrams (bidirectional data) of orientation were determined by using VectorRose 3.02 software (PAZ Software).

Time-Lapse Analysis

Dechorionated embryos were mounted in a mixture of 1.5% low melting point agarose (FMC BioProducts; SeaPlaque, gelling temperature of 1.5% solution, 26–30°C) and 0.75% methylcellulose in Normal Ringer's solution (Westerfield, 1996) and oriented ventral side up on coverslip-bridged slides. Images were collected at 30-s intervals with an Axiophot2 microscope, an Axiocam digital camera, Axiovision software (Zeiss), and a Dimension XPS 800 MHz Pentium III computer with 256 MB SDRAM (Dell). Images were analyzed with NIH Image (Wayne Rasband) and Object-Image (Norbert Vischer) software on Macintosh computers. Time-lapse recordings proceeded for 10 to 40 min at 24–28°C. Neighbor exchanges were calculated for cells that could be followed throughout the time lapse. Net paths were plotted with VectorRose 3.02 software (unidirectional data).

RESULTS

Three Domains of Convergence and Extension Movements in the Zebrafish Gastrula

Convergent extension movements, which lead to the narrowing and lengthening of cell populations, are best understood in *Xenopus*, based on experiments with tissue explants (reviewed in Keller *et al.*, 2000). To address this process in the intact embryo, we used two basic assays for quantifying CE movements in the translucent zebrafish gastrulae. Through morphometric analyses, the narrowing of somitic and midline tissue (convergence) and the anterior–posterior (AP) lengthening of midline tissues and the embryonic axis (extension) can be directly observed. Tissue convergence and extension are also reflected by the movements and rearrangements of small cell populations. Injections of lipophilic dyes into the blastoderm margin at the beginning of gastrulation (6 hpf) mark predominantly ectodermal cells, whereas activation of caged fluorescein

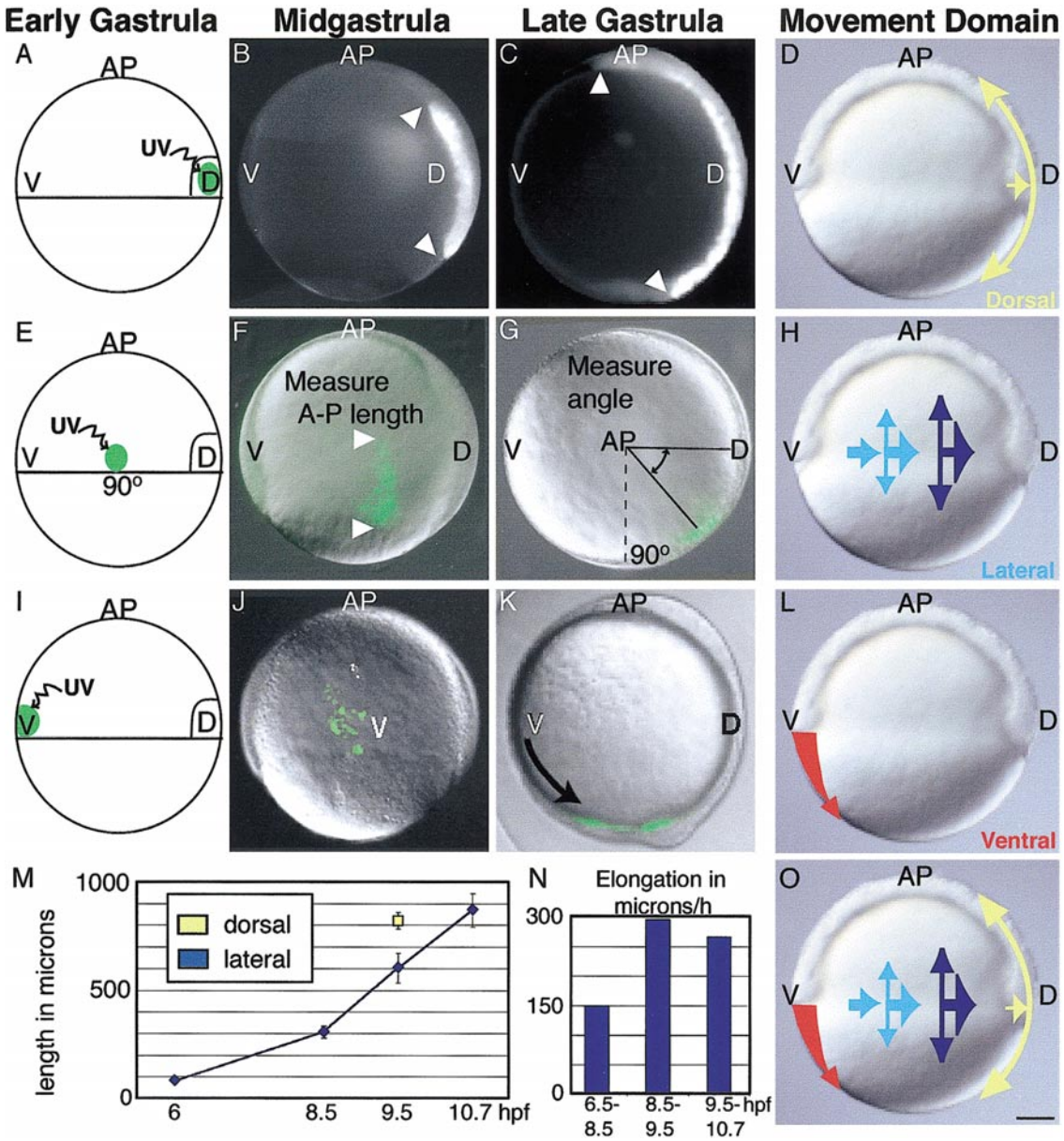

FIG. 1. Domains of distinct convergence and extension movements in the zebrafish gastrula. The movements of groups of mesendodermal cells were examined in three regions: (A) dorsal, (E) lateral, and (I) ventral. Cells were labeled by photoactivation of a caged fluorescein dye. Resulting labeled cell arrays are illustrated at midgastrulation (8.5 hpf; B, F, J) and at the end of the gastrula period (9.5 hpf; C, G, K). (B, C, F) Elongation of dorsal and lateral cells groups was measured to monitor extension movements (M), and the rate of elongation of lateral cell arrays is shown in (N). (G) Dorsalward translocation of lateral cells was measured to monitor convergence. (I) Labeled cells of the ventral margin in WT gastrulae move underneath ectoderm and spread over the yolk (J), then into the tailbud region (K). From these and previous experiments (Sepich *et al.*, 2000), three movement domains are inferred: (D) a dorsal region of strong extension and moderate convergence (yellow arrow), (H) a lateral domain of increasing convergence and extension (light blue to dark blue arrows), and (L) a ventral domain of inhibited convergence and extension (red arrow). This model is summarized in (O). Scale bar, 100 μm.

largely labels mesodermal cells (Sepich *et al.*, 2000). Dorsal translocation of the labeled cells along the equator is measured to assay convergence, whereas the anteroposterior dimension of the resulting cell array is measured to quantify extension movements (Figs. 1F and 1G). Our previous studies revealed that the speed of dorsal translocation of lateral cell groups is slow at first, increasing to a peak as they move toward dorsal, and slowing down again

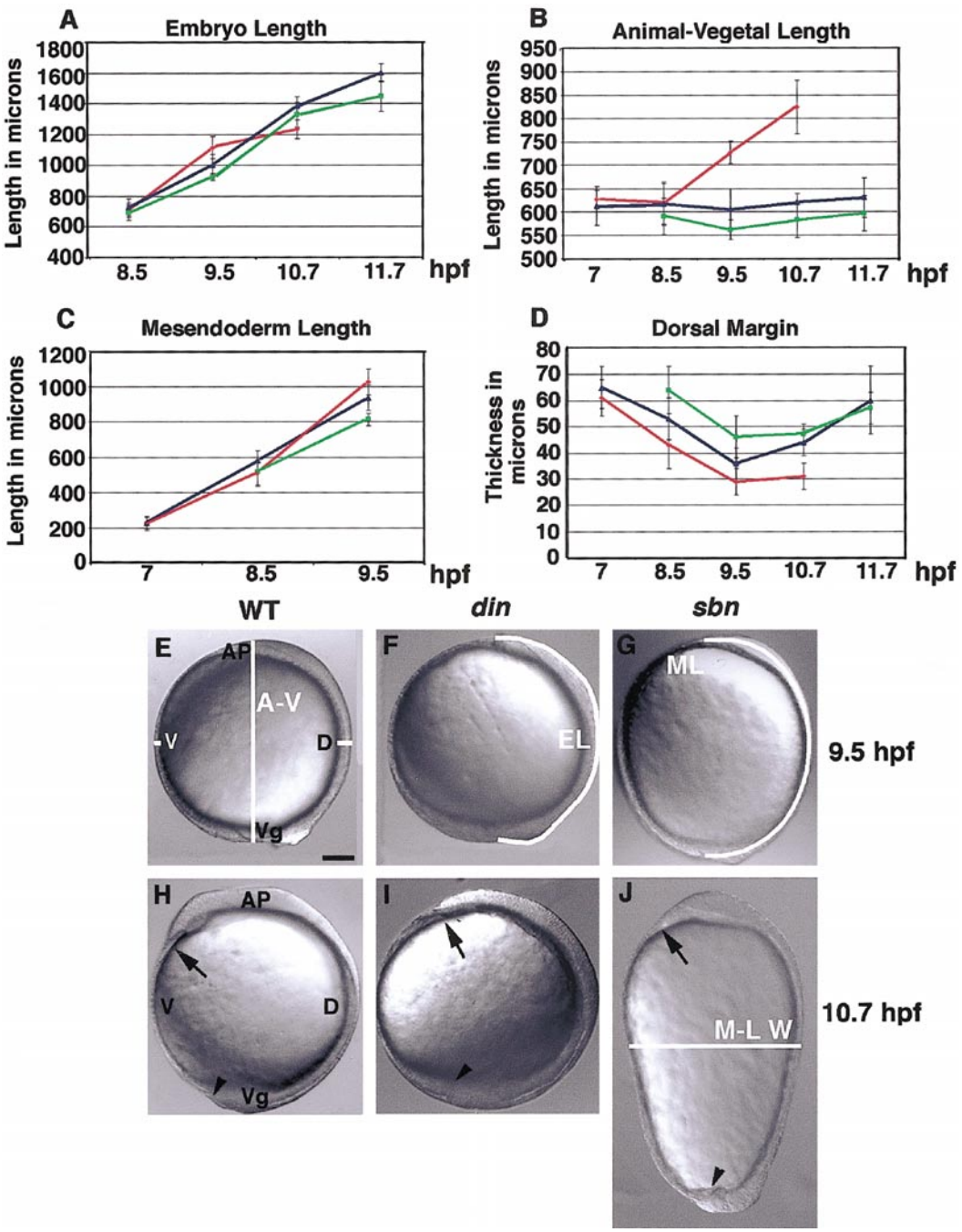

FIG. 2. Increase and decrease in Bmp activity have distinct effects on CE of tissues and embryonic morphology. Graphs showing results of morphometric analysis of WT (blue), *sbn* (red), and *din* (green) mutant embryos: (A) embryo length, (B) animal–vegetal length, (C) dorsal mesendodermal length, and (D) thickness of dorsal margin. (E) Lateral view of a WT embryo at the end of the gastrula period (9.5 hpf) with animal pole (AP), vegetal pole (Vg), ventral (V), and dorsal (D) marked. The dorsal and ventral margin thickness and the animal–vegetal dimension are shown. (F) *din* embryo at 9.5 hpf; embryo length measure is shown. (G) *sbn* embryo at 9.5 hpf; mesendodermal length measure is indicated (ML). (H) WT, (I) *din*, and (J) *sbn* embryos at the beginning of segmentation; mediolateral embryo width is indicated (M-LW; 10.7 hpf). Arrows denote anterior tip of mesendoderm, and arrowheads mark tail region (H–J). A–V, animal–vegetal length; EL, embryo length; ML, mesendoderm length; M-LW, mediolateral width. Scale bar, 100 μm.

as these lateral cells approach the dorsal midline (Sepich *et al.*, 2000).

To determine whether extension movements also increase from lateral to dorsal regions, we labeled cell groups located 90° from (Fig. 1E) and at the dorsal midline (Fig. 1A) and measured the AP length of the resulting cell arrays (Figs. 1B, 1C, 1F, and 1M). Over time, these cell arrays become interrupted as labeled and unlabeled cells intercalate between one another (Kimmel *et al.*, 1994). The labeled lateral cell groups elongate slowly at first and then speed up after midgastrulation (Figs. 1M and 1N). Furthermore, we found that similarly labeled dorsal cell groups elongate more than lateral cell populations (Fig. 1M). Together with previous analysis of convergence movements (Sepich *et al.*, 2000), these observations indicate that the lateral gastrula region constitutes a domain of increasing convergence and extension movements (Fig. 1H). By contrast, dorsal cell groups strongly extend while only moderately converging (Fig. 1D).

Movements in the ventral region may differ from the dorsal and lateral domains described above since fate-mapping analyses indicate that the ventral-most cells contribute to the tail (Kanki and Ho, 1997; Kimmel *et al.*, 1990). We found that cells labeled at the ventral margin (Fig. 1I) did not move dorsally, but initially spread over the yolk and later moved into the tailbud region (Figs. 1J and 1K). Such spreading movement, followed by migration toward the vegetal pole, was observed for cell groups residing in a 20–30° arc of the ventral margin ($n = 56$, see Fig. 4A), a domain we designate as the no convergence no extension zone (NCEZ).

Collectively, these studies demonstrate that the speed and magnitude of convergence and extension movements differ along the dorsoventral axis. Three morphogenetic domains are defined in the zebrafish gastrula: a ventral (NCEZ) domain in which convergence and extension do not occur, a lateral domain of increasing convergence and extension, and a dorsal domain of strong extension with little convergence (summarized in Fig. 1O). We hypothesized that Bmp activity plays a role in specification of these morphogenetic domains.

Morphometric Analysis Reveals a Role of Bmp Activity in Modulation of Convergent Extension

To begin elucidating how Bmp activity modulates CE, we examined the morphology of WT as well as ventralized *chordino* (*chordin, din*) and dorsalized *somitabun* (*smad-5, sbn*) mutant embryos. In *din* mutants, the inactivation of a Bmp antagonist results in a dorsal expansion of Bmp activity (Hammerschmidt *et al.*, 1996; Schulte-Merker *et al.*, 1997), while in *sbn* mutants, loss of the downstream effector leads to a decrease in Bmp signaling (Hild *et al.*, 1999).

Extension of tissues is evidenced by the gradual increase in AP length of the embryo and the nascent dorsal mesendoderm (Sepich *et al.*, 2000). By midgastrulation, *din* embryos exhibited a reduced mesendoderm length (WT, 583 ± 57 μm; *din*, 516 ± 81 μm, 8.5 hpf, $P = 0.039$; Fig. 2C), which was more severely compromised by the end of the gastrula period (WT, 923 ± 66 μm; *din*, 813 ± 34 μm, 9.5 hpf, $P = 2.8 \times 10^{-6}$; Figs. 2C, 2E, and 2F). Additionally, the length of the embryonic axis in *din* mutants was shorter relative to WT at both the end of the gastrula period (Fig. 2A) and the early segmentation stage (WT, 1387 ± 57 μm; *din*, 1175 ± 86 μm, 10.3 hpf; Figs. 2A, 2H, and 2I) revealing an extension defect.

The thickness of the dorsal blastoderm margin can be increased by convergence and decreased by extension and epiboly movements. The dorsal margin in *din* mutants thinned less compared with WT siblings during gastrulation, whereas analysis of *sbn* mutants revealed that the dorsal margin was thinner by midgastrulation (Fig. 2D). In WT embryos, the ventral margin thins as cells migrate dorsally or to the tail (Sepich *et al.*, 2000). The ventral margin was thicker in *din* and *sbn* by the end of the gastrula period (data not shown). During normal gastrulation, a cell-depleted evacuation zone in the ventro-animal region of the embryo forms as ventral and lateral animal cells move dorsally through convergence and vegetally by epiboly (Kimmel *et al.*, 1995). This zone is clearly visible by the onset of segmentation in WT yet was reduced in both ventralized *din* and dorsalized *sbn* mutants, indicating a convergence and/or epiboly defect consistent with the increased thickness of the ventral margin (data not shown).

The elongated *sbn* gastrula shape, characteristic of dorsalized embryos (Mullins *et al.*, 1996), was reflected by the increased animal–vegetal embryonic axis and dorsal mesodermal lengths by the end of gastrulation (Figs. 2A, 2B, 2C, and 2G). However, while animal–vegetal length continued to increase (WT, 620 ± 20 μm; *sbn*, 825 ± 57 μm; Fig. 2B), the length of the *sbn* embryonic axis became shorter relative to WT by early segmentation (WT, 1387 ± 57 μm; *sbn*, 1235 ± 61 μm; Figs. 2A, 2H, and 2J). In WT embryos, the head rudiment advanced around the yolk at this stage, but the *sbn* head rudiment was stalled at the animal pole (Figs. 2H and 2J). Further measurements revealed that the distance from the anterior tip of the head to the first somite cleft was shorter in *sbn* compared with WT (WT, 748 ± 40 μm, $n = 10$; *sbn*, 644 ± 39 μm, $n = 9$), indicating defective extension of anterior tissues of *sbn* mutants at this stage.

These findings reveal the critical role of convergent extension in shaping the embryonic body since epiboly and involution/ingression movements do not appear grossly affected in *din* and *sbn* mutant gastrulae (Mullins *et al.*, 1996, and see below). These morphometric analyses directly demonstrate convergence and/or extension defects of some tissues in *sbn* and *din*. However, it is unclear whether abnormalities in the thickness of marginal tissues are due to changes in convergence, extension, or epiboly movements, which we addressed by analyzing movements of cell populations.

Elongation of Dorsal and Lateral Cell Groups Is Reduced in Ventralized Mutants

To determine the effect of Bmp activity on extension movements of dorsal cell populations, small (80 ± 3 μm, $n = 14$) groups of cells were labeled in the embryonic shield (6 hpf) of ventralized *din* and dorsalized *sbn* mutants by photoactivation of caged fluorescein dye (Kozlowski *et al.*, 1997). At the end of the gastrula period (9.5 hpf; Fig. 1), we observed no difference in anteroposterior length of the labeled ectodermal cell arrays between WT and mutant embryos (Fig. 3A). However, the length of the labeled mesendodermal cell array in *din* mutants (664 ± 39 μm, $n = 11$) was reduced to 81% of WT length (821 ± 38 μm, $n = 13$, $P = 2 \times 10^{-9}$; Fig. 3A). By contrast, the length of the labeled dorsal mesendoderm in *sbn* mutants was not significantly different from that of WT (842 ± 50 μm, $n = 16$, $P = 0.21$). Thus, extension of dorsal mesendodermal cell groups was suppressed in embryos with dorsally expanded Bmp activity but not in those with less Bmp signaling, consistent with reduced mesendoderm and embryonic axis length in *din* embryos and normal respective dimensions in *sbn* mutants at this stage of development (Figs. 2A and 2C).

Our previous fate mapping studies demonstrated that extension is similarly affected in lateral mesendodermal cell groups since elongation is extremely reduced in ventralized mutants compared with WT (Sepich *et al.*, 2000; Figs. 3C and 3D). Conversely, in *sbn*, the length of the labeled cell array did not appear significantly smaller than WT and may be increased (Fig. 3E). Together, these studies show that high Bmp activity inhibits, and low Bmp activity permits, extension movements.

Dorsal Translocation of Lateral Cells Is Impaired in Ventralized and Dorsalized Mutants

To learn how Bmp activity regulates convergence movements, we labeled marginal cell groups, 90° from the dorsal midline, of WT, ventralized, and dorsalized mutant gastrulae with a lipophilic dye as gastrulation began and tracked their dorsal translocation (Figs. 1E–1G). Through midgastrulation (8.5 hpf), lateral marginal cells in *din* and *sbn* mutant embryos moved normally toward the dorsal midline (WT, 75 ± 7°, $n = 60$; *sbn*, 76 ± 5°, $n = 16$; *din*, 76 ± 10°, $n = 10$). However, by the end of the gastrula period (9.5 hpf), dorsal movement of labeled cell populations in both dorsalized and ventralized mutants was reduced (WT, 51 ± 9°, $n = 68$; *sbn*, 67 ± 7°, $n = 16$, $P = 5.7 \times 10^{-6}$; *din*, 61 ± 12°, $n = 12$, $P = 0.001$; Fig. 3B). Thus, in zebrafish, both an expansion and a deficit of Bmp activity impair dorsalward movements of lateral marginal cells, supporting the notion that the increasing speed of convergence documented in the lateral domain of WT embryos (Trinkaus *et al.*, 1992; Sepich *et al.*, 2000) is dependent on moderate levels of Bmp activity.

High Bmp Activity Specifies the Ventral No Convergence and No Extension Morphogenetic Domain

We have shown that cells occupying a 20–30° arc of the ventral gastrula margin ($n = 56$; Fig. 4A), which are exposed to the highest level of Bmp signaling (Dosch *et al.*, 1997; Nguyen *et al.*, 1998; Nikaido *et al.*, 1997; Wilson *et al.*, 1997), failed to converge dorsally but rather involuted, spread over the yolk during gastrulation, and subsequently moved into the tailbud (Figs. 1J and 1K). We reasoned that, if high levels of Bmp specified this behavior, then the NCEZ should be expanded in ventralized mutants. Indeed, labeling of the marginal cell groups in *din* mutants showed that the NCEZ was broadened to a 60–70° arc of the ventral margin ($n = 26$; Fig. 4B).

The size of the NCEZ was also assessed in *bozozok*$^{m168/m168}$ *chordino*$^{tt250/tt250}$ (*boz din*) double mutants, in which the combined inactivation of a negative regulator of Bmp and a Bmp antagonist leads to a dramatic dorsal expansion of the ventral domain of high Bmp activity and consequent loss of head and trunk (Gonzalez *et al.*, 2000). Since the embryonic shield, which identifies the dorsal side, does not form in *boz din* mutant gastrulae, at least two groups of marginal cells were randomly labeled and the embryos were fixed at the end of gastrulation (9.5 hpf). At this time in *boz din* double mutants, the majority of cells have accumulated in the vegetal region of the embryo, and they express the mesodermal marker *paraxial protocadherin* (*papc*) (Gonzalez *et al.*, 2000). We found that all labeled marginal cell populations in double mutants failed to translocate away from the spot of their original labeling, indicating an inhibition of convergence. Moreover, they failed to extend but moved vegetally, eventually residing within the *papc* expression domain ($n = 7$, Figs. 4C and 4D). This is in contrast to WT, *din*, and *sbn*, where labeled dorsolateral cell groups extend anterior of the *papc* domain (Fig. 3C). This vegetal movement without convergence or extension was observed in labeled cell populations located at the blastoderm margin as far as 180° apart. These data further support the notion that high levels of Bmp activity inhibit convergence and extension.

Dorsal expansion of Bmp activity could inhibit convergence extension movements by limiting dorsal signals promoting these movements and/or by impacting ability of these ventral cells to receive or respond to such signals. To distinguish between these possibilities, we transplanted prospective mesodermal cells from donors overexpressing a constitutively active type I Bmp receptor (CA-BRIA) into the blastoderm margin of WT hosts. Previous studies demonstrated that, within ectoderm, CA-BRIA could promote nonneural cell fates in a cell-autonomous manner (Nikaido *et al.*, 1999). Following transplantation at late blastula stages (4–5 hpf), the position of the cells relative to dorsal was determined at the beginning of gastrulation. The anteroposterior position and array elongation were then assessed at the end of the gastrula period. In addition, expression of *six3* and *papc* was analyzed in these embryos by *in*

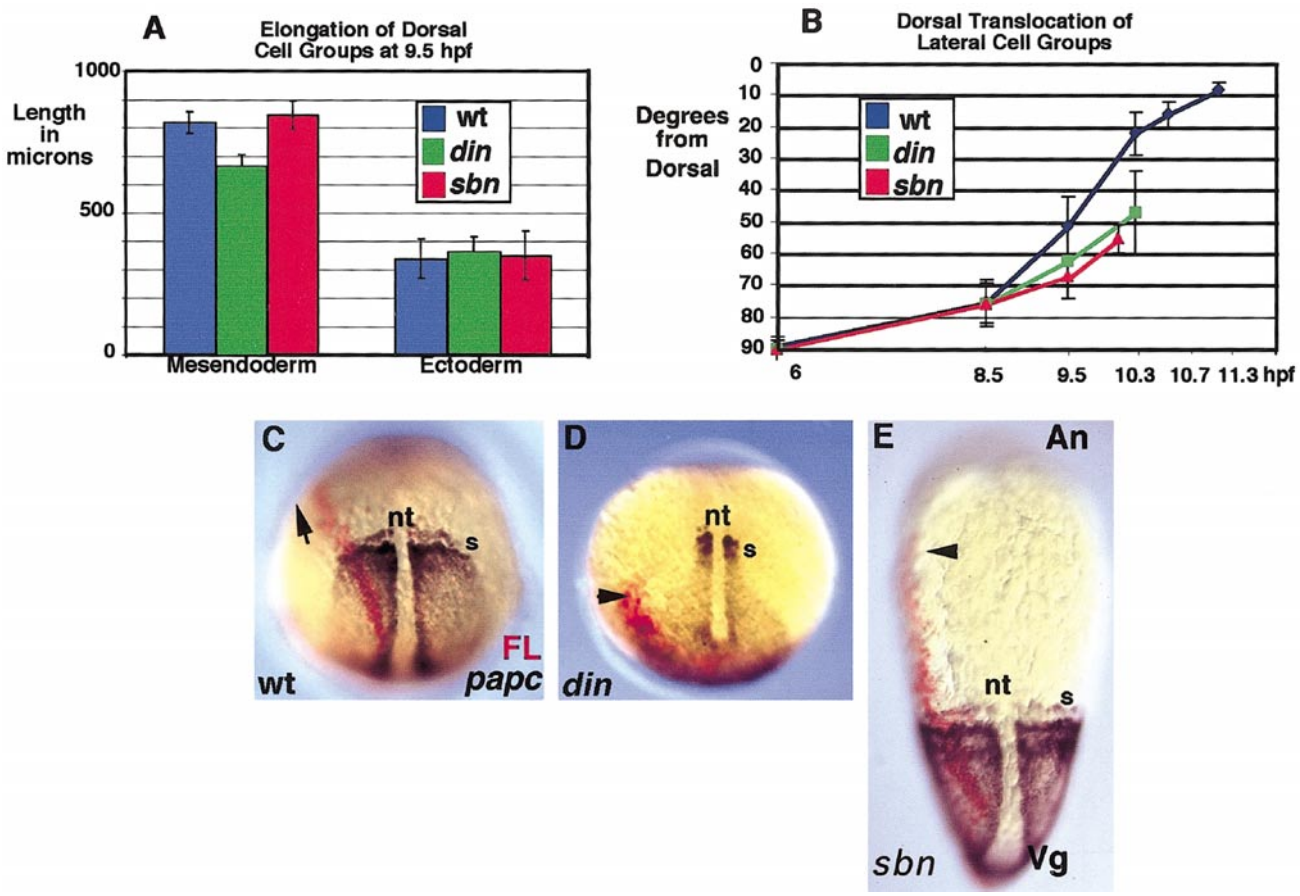

FIG. 3. Elongation of dorsal mesendodermal cell populations, dorsal translocation, and fate-mapping analyses of lateral cell groups in WT, *din*, and *sbn* mutants. (A) Elongation of labeled mesendodermal cell populations is reduced in *din* mutant gastrulae by the end of the gastrula period. (B) Assaying dorsal translocation of labeled lateral marginal cells indicates that convergence movements in both *sbn* and *din* mutants become impaired after midgastrulation. Fate-map analysis of lateral marginal cells in (C) WT, (D) *din*, and (E) *sbn* embryos at early segmentation; the resulting labeled lateral cell array is seen in red (FL). The anterior boundary of the labeled cell array is marked by an arrowhead; in WT, the array extends around the embryo into the head mesoderm and its anterior boundary is not visible, denoted by an arrow. *paraxial protocadherin* (*papc*) expression is shown in brown. s, somites; n, notochord.

situ hybridization, while transplanted cells were visualized by antibody staining. Cells transplanted from uninjected donors or from donors that were not significantly ventralized by CA-BRIA overexpression underwent significant anteroposterior elongation when transplanted into dorsolateral regions of WT hosts as expected from cell labeling studies described above (compare Fig. 3C with Figs. 4E and 4G; $n = 11$). By contrast, mesodermal cells transplanted from strongly ventralized donors, as evidenced by very reduced or absent *six3* expression and vegetally expanded *papc* expression (Gonzalez *et al.*, 2000), formed short cell arrays confined to the posterior trunk or tailbud region regardless of their original position within the gastrula (Figs. 4F and 4H; $n = 9$). Thus, the cell groups overexpressing CA-BRIA show very limited extension movements as observed for cell populations residing within the ventral NCEZ (Fig. 1K). The host embryos exhibited normal morphology and *papc* expression, indicating that the transplanted cells overexpressing CA-BRIA have limited influence on neighboring cells, as observed previously (Nikaido *et al.*, 1999). This result argues that high levels of Bmp are sufficient to inhibit extension and promote vegetal migration in a cell-autonomous manner.

High Levels of Bmp Are Necessary for NCEZ Formation and Promote Vegetal Migration

If high levels of Bmp activity specify the NCEZ, then this domain should be absent from dorsalized *sbn* embryos. Accordingly, labeled ventral marginal cells of *sbn* gastrulae formed arrays elongated in the animal–vegetal axis instead of migrating to the tail by the end of the gastrula period

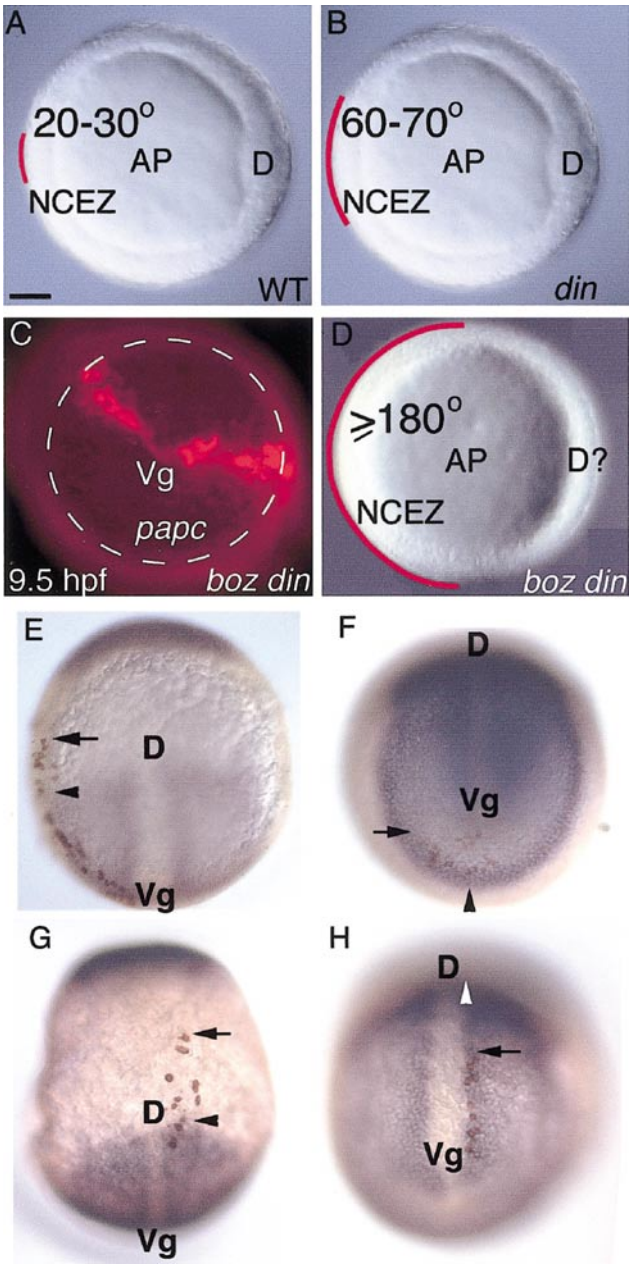

FIG. 4. The NCEZ is specified by high levels of Bmp activity. (A) In WT, the NCEZ comprises 20–30° of the ventral margin. (B) The dorsally expanded Bmp activity in moderately ventralized *din* mutants leads to an enlargement of the NCEZ to a 60–70° arc of the ventral margin. (C) Further dorsal expansion of Bmp activity in *boz din* double mutants results in a dramatic NCEZ enlargement. Shown is a vegetal view of a *boz din* embryo, with a broken line marking the enlarged vegetal *papc* expression domain. Labeled cells moved into this vegetal region without translocating dorsally away from their original point of labeling. Furthermore, they fail to extend beyond the *papc* expression domain. (D) Cells from at least a 180° arc of the ventral margin constitute NCEZ in *boz din* mutants. (E) Dorsal view of a host embryo at the end of the gastrula period with transplanted cells (in brown) from a nonventralized host. At the beginning of gastrulation, the transplanted cells were in the ventral lateral region of the margin. (F) Cells that were transplanted from a strongly ventralized donor to the same ventral lateral region of the gastrula have moved into the tailbud region, shown in this vegetal view. (G) Dorsal view of cells transplanted from a nonventralized donor near the dorsal shield at the beginning of the gastrula period. They form arrays extending outside of the *papc* expression domain. (H) Dorsovegetal view of a host embryo with cells from a ventralized donor that were transplanted near the dorsal shield and have now moved into the posterior trunk and tailbud region.

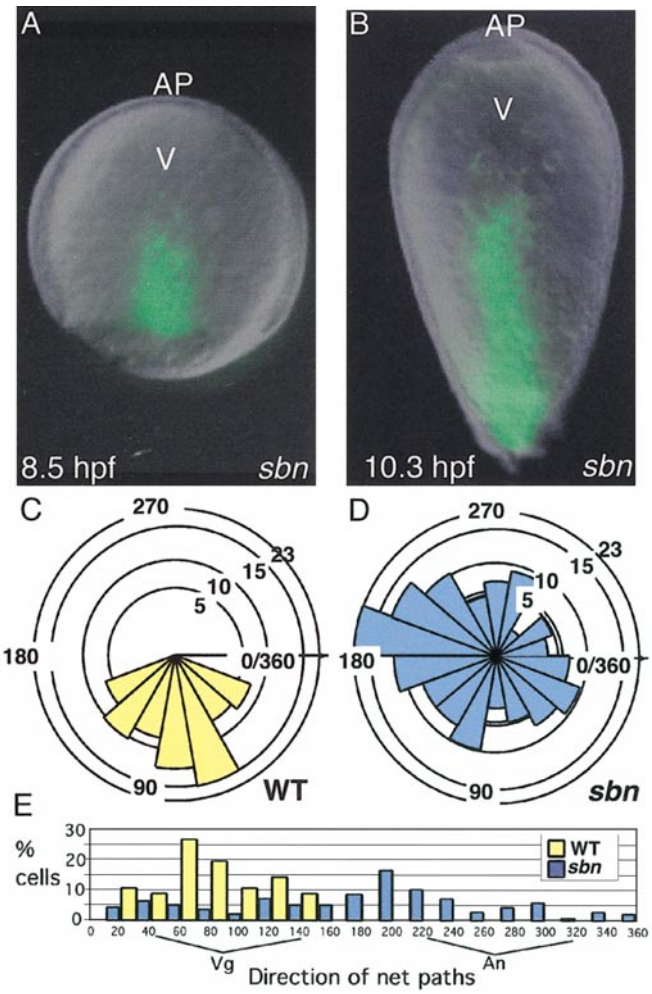

FIG. 5. High levels of Bmp activity are necessary for NCEZ and promote vegetal migration of mesendodermal cells. (A) Ventral view of a labeled *sbn* embryo at midgastrulation; note the extended cell array. (B) *sbn* embryo at early segmentation showing a significantly elongated labeled cell array. (C) Ventral cells migrate vegetally in WT from mid- to late gastrulation. The direction of their net paths was determined from three time-lapse recordings from 8.2 to 8.8 hpf (75–85% epiboly). Rose diagrams are arranged to represent the number of ventral cells taking these net paths, with all paths starting at a common origin; vegetal is represented as 90° and animal direction as 270°. (D) Ventral mesodermal cells in *sbn* migrate along net paths oriented in all directions. (E) The same data are represented as the percentage of cells taking each net path, in order to demonstrate the strong vegetal bias in WT and slight lateral bias in *sbn*. Scale bar, 100 μm.

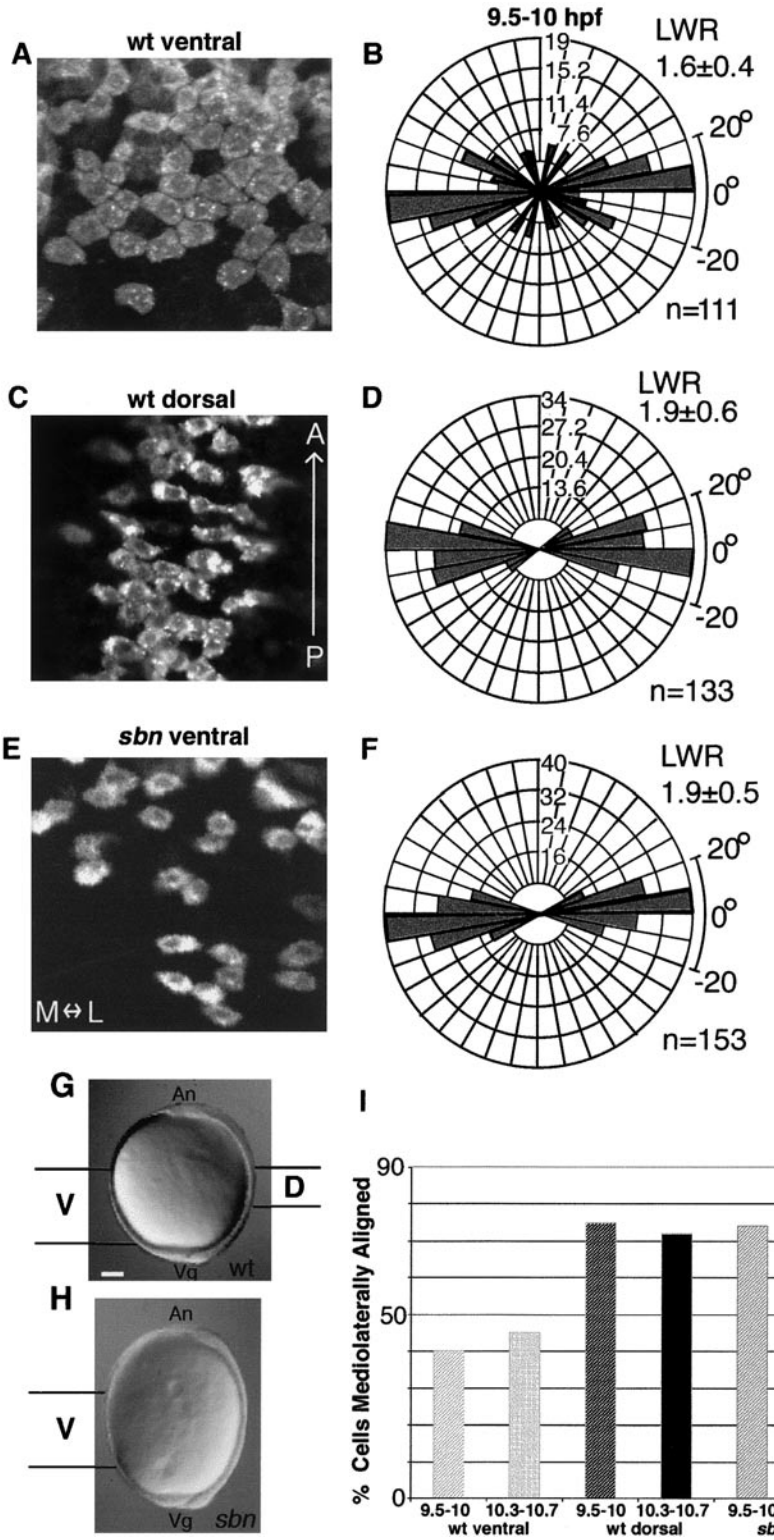

(Figs. 5A and 5B). In *sbn* mutants, cell groups within 90–100° of the ventral margin elongated anteroposteriorly without strong dorsal translocation ($n = 25$). From the observations that NCEZ is proportionally enlarged in ventralized while absent in dorsalized mutants and that overexpression of a CA-BRIA cell-autonomously inhibits extension while promoting vegetal migration, we conclude that a high threshold of Bmp activity observed in the ventral region of WT embryos is necessary and sufficient for specification of this morphogenetic domain.

To understand what cell behaviors are influenced by Bmp activity so that WT but not all *sbn* ventral cells migrate toward the tailbud, we performed time-lapse microscopy analysis of the ventral region at midgastrulation stages (8.2–8.8 hpf). In WT embryos, ventral mesendodermal cells move as individuals, with net paths oriented vegetally (Fig. 5C; $n = 56$ cells in three time lapses, 8.2–8.8 hpf, midgastrulation). There is substantial meandering mediolaterally ($M_x = 6.3 \pm 6.8$; M_x = total path in mediolateral direction/net path in mediolateral direction ± standard deviation). By contrast, these cells meander little in the animal–vegetal (AnVg) axis ($M_y = 1.8 \pm 1.0$; M_y = total path in AnVg direction/net path in AnVg direction ± standard deviation), suggesting that the cues guiding the vegetal migration are strong, while mediolateral movement is not directed. Similar analyses of the ventral region in *sbn* showed that, initially, *sbn* cells behave normally upon internalization, spreading over the yolk during early gastrulation like WT cells (Fig. 5A). However, *sbn* cells do not migrate vegetally at the appropriate time. Instead, at midgastrulation stages, these cells can migrate in any direction (Fig. 5D; $n = 139$ cells in four time lapses, 8.2–8.8 hpf). These observations further demonstrate that, in addition to inhibiting convergence and extension movements, high Bmp activity levels promote a vegetalward migration of mesodermal cells during midgastrulation stages. They also indicate that, during gastrula stages, *sbn* cells form elongated arrays because some mutant cells fail to undergo vegetalward migration.

Mediolateral Cell Elongation at Low Levels of Bmp Activity

We have shown that high levels of Bmp activity inhibit convergence and extension while promoting vegetalward migration of cells. Consistent with this notion, ventral cell populations in *sbn* do not move to the forming tailbud during midgastrulation. To elucidate the cell behaviors associated with low Bmp activity at later stages of gastrulation, we analyzed cell orientation and morphology in ventral and dorsal regions of WT gastrulae and in ventral regions of *sbn* gastrulae. Mediolateral alignment and elongation of cells have been correlated with CE movements in *Xenopus* and zebrafish (Concha and Adams, 1998; Keller *et al.*, 1985; Wallingford *et al.*, 2000; Topczewski *et al.*, 2001). We injected a lipophilic dye, DiI, into a single cell of 8- to 16-cell-stage WT or *sbn* mutant embryos (Cooper *et al.*, 1999). By the gastrula stage, labeled cells became scattered throughout ectoderm and mesendoderm. Using confocal microscopy, we acquired images of ectodermal and mesodermal cell populations at the end of the gastrula period (9.5–10 hpf) and at the beginning of segmentation, when considerable axis extension is observed (10.3–10.7 hpf, see *Materials and Methods;* Figs. 6A, 6C, and 6E). Orientation of the long axis of a cell relative to the mediolateral axis of the embryo and their length to width, or aspect, ratio (LWR) was calculated.

We observed that, in the dorsal region adjacent to the forming notochord, the majority of ectodermal and mesodermal cells were mediolaterally aligned at the end of the gastrula period (73%, $n = 133$ cells) and at the beginning of segmentation (72%, $n = 78$, axes orientation from 180–160° and 0–20°; Figs. 6D and 6I). These cells were highly elongated, since their average LWRs were 1.9 ± 0.6 and 2.1 ± 0.6, respectively (Fig. 6D, and data not shown). In contrast, ventrally, where convergence and extension movements do not occur and Bmp activity is high, less than half the ectodermal and mesodermal cells were mediolaterally aligned (39%, $n = 111$; 9.5–10 hpf; 45%, $n = 133$; 10.3–10.7 hpf; Figs. 5B and 5I). Moreover, ventral cells were not as elongated as their dorsal counterparts (LWR, 1.6 ± 0.4, $P = 2.5E^{-}7$; 1.7 ± 0.5, $P = 0.0004$; Fig. 6B). These findings correlate low levels of Bmp activity on the dorsal side (Fig. 1D) with a high degree of mediolateral cell alignment and elongation, typical of cells involved in intercalation (Wallingford *et al.*, 2000; Keller *et al.*, 1985). We tested whether low Bmp activity levels could specify mediolateral alignment and elongation of cells by examining cells in the ventral region of *sbn* gastrulae. The majority of cells were mediolaterally aligned at both the end of the gastrula period (73%, $n = 154$; 9.5–10 hpf) and the beginning of segmentation (83%, $n = 128$; 10.3–10.7 hpf; Figs. 6F and 6I). Moreover, *sbn* cells were also elongated compared with WT ventral cells (LWR, 1.9 ± 0.5, $P = 4.3 \times 10^{-7}$;

FIG. 6. Cells at low levels of Bmp activity are mediolaterally aligned and elongated. Confocal microscope images of DiI-labeled cells from (A) WT ventral, (C) WT dorsal, and (E) *sbn* ventral regions (9.5–10.3 hpf). (B, D) Rose diagrams of cell orientations from WT and (F) *sbn* embryos at 9.5–10 hpf. The mediolateral axis corresponds to the horizontal plane, while the anteroposterior axis aligns vertically. Cell number scale is indicated on each diagram. (G, H) An overview of the locations of cells analyzed in WT and *sbn* embryos. (I) Graph shows percentage of analyzed cells, which are mediolaterally aligned, i.e., orient the long axis ± 20° with respect to the mediolateral axis. Hatched bars indicate late gastrula stages (9.5–10 hpf); solid bars are early segmentation stages (10.3–10.7 hpf). *n*, number of cells analyzed; LWR, length/width ratio. Scale bar, 100 μm.

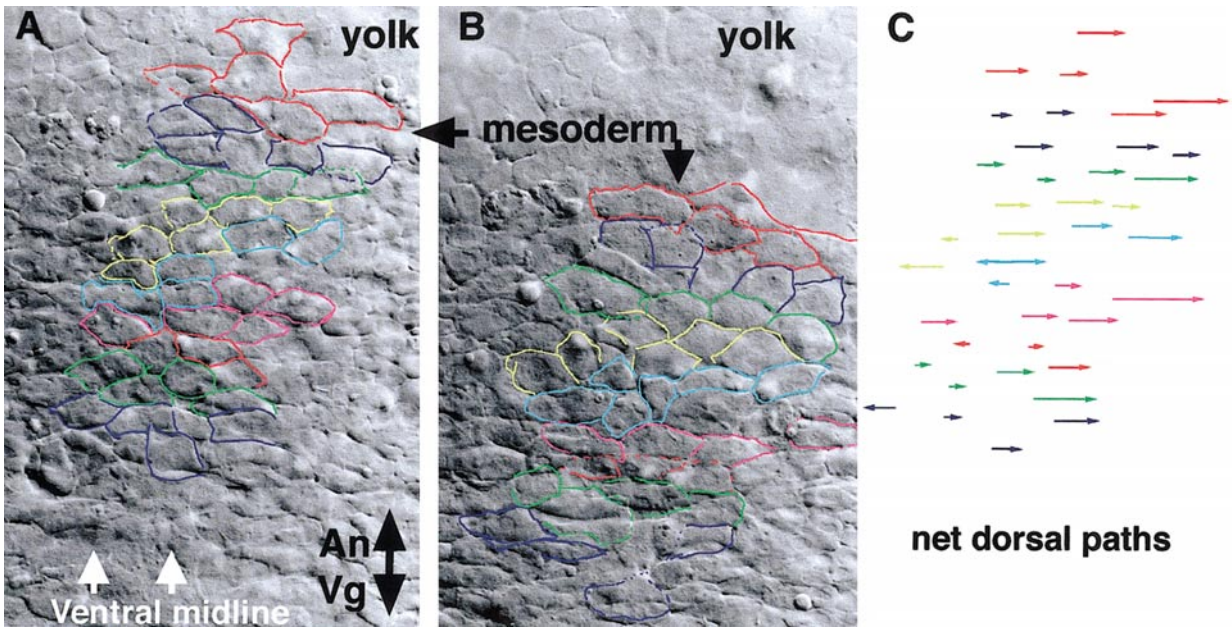

FIG. 7. Dorsally biased mediolateral intercalation in ventral regions of *sbn* mutants. Time-lapse Nomarski image recordings were made of ventral mesodermal cells in *sbn* embryos beginning shortly after the end of the gastrula period (9.7 hpf) until the beginning of segmentation (10.3 hpf). (A) Initial image showing mesodermal cells overlaying the yolk, vegetal pole to the bottom. Cells that could be identified throughout the recording are outlined in color. (B) After 40 min, the analyzed cell population moved vegetally, with respect to the yolk. Individual cells intercalated, dorsally broadening the population in a mediolateral direction. The corresponding net path of each cell is shown in (C).

2.0 ± 0.5, $P = 4.2 \times 10^{-8}$; Fig. 6F, and see above), thus correlating ectopic mediolateral cell elongation with ectopic extension movements (Figs. 5A and 5B).

Ectopic Dorsally Biased Intercalation of Ventral sbn Cells at the End of Gastrulation

During the period from the end of gastrulation through early segmentation, the animal–vegetal length of *sbn* embryos increases while their dorsoventral dimension narrows (Fig. 2B, D–V embryo width 590 ± 50 μm, 9.5 hpf, 519 ± 48 μm, 10.7 hpf; $P = 0.006$), so that, in effect, the entire embryo converges and extends. In contrast, WT embryos do not narrow at this time (565 ± 24 μm, $n = 9$, 9.5 hpf, 571 ± 21 μm, $n = 10$, 10.7 hpf; $P = 0.59$). As described above, ventral mesodermal *sbn* cells fail to migrate vegetally, forming cell arrays, elongated in the animal–vegetal axis (Figs. 4E–4I). These cells become mediolaterally elongated at late gastrula and early segmentation, similar to WT dorsal cells, but in contrast to WT ventral cells (Fig. 6). To characterize the behavior of these ventral mesodermal cells in *sbn* at late gastrula and early segmentation stages, we performed time-lapse analyses. In three time-lapse movies, the analyzed cells moved primarily vegetally but also dorsally (Fig. 7; $n = 149$). Therefore, in *sbn*, as the entire embryonic tissue converges (Fig. 2J), the ventral cell populations undergo mediolateral divergence, i.e., spread dorsally. The individual cells within the population do not intercalate toward a ventral midline, but rather dorsally, making a conservative number of neighbor exchanges (2 per cell per hour; $n = 6$ cells) similar to what has been calculated for deep neural over mesoderm frog tissue explants (Elul *et al.*, 2000). Mediolateral divergence of cell populations appears to increase slightly over time, and chains of mediolaterally elongated cells are visible (Figs. 7A and 7B). These observations are consistent with ventral mesodermal *sbn* cells engaging in dorsally directed intercalation, which we predict would create a posterior constrictive force and would account for narrowing the embryo in the mediolateral (dorsoventral) axis (Fig. 2J). Preliminary results indicate that the intercalation of ventral *sbn* cells described above began after the end of the gastrula period (D.S.S. and L.S.K., unpublished observations), when mediolateral narrowing of the *sbn* gastrula occurs, as described above. Based on these analyses of population movements and cell behaviors, we suggest that low levels of Bmp activity in dorsalized mutants allow the expansion of the dorsal domain of generous extension with little dorsal convergence, driven by dorsally directed intercalation, around the circumference of the late gastrula (see Fig. 9H).

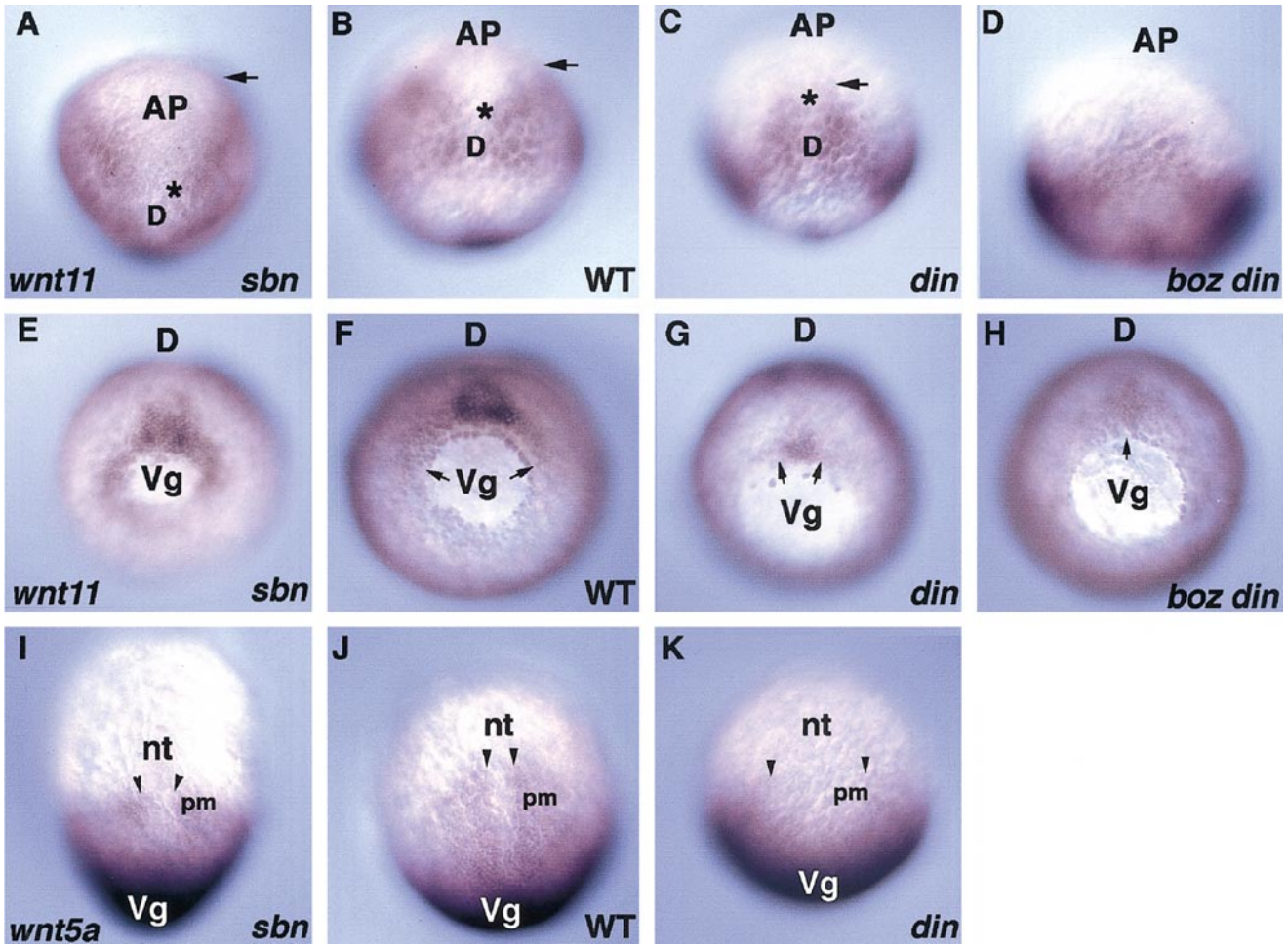

FIG. 8. *wnt11* (*slb*) (A–H) and *wnt5a* (*ppt*) (I–K) expression patterns during late gastrulation (9–9.2 hpf). (A–H) Asterisks denote dorsal boundary of anterior *wnt11* expression domain, while arrows indicate ventral boundary. (A) Dorsoanterior view of *sbn* gastrulae showing ventrally expanded expression of *wnt11.* Dorsal views of (B) WT, (C) *din,* and (D) *boz din* embryos showing progressive reduction of the anterior *wnt11* expression domain in the ventralized mutants. Vegetal views of (E) *sbn,* (F) WT, (G) *din,* and (H) *boz din* embryos showing expansion in dorsalized and reduction in ventralized mutants of the *wnt11* expression domain near the blastopore. Lateral boundaries of the blastopore expression are marked by arrows. Dorsal views of (I) *sbn,* (J) WT, and (K) *din* embryos showing *wnt5a* expression in presomitic mesoderm in *sbn* and WT and its loss in ventralized *din* mutants. Dorsal limits of expression are indicated by arrowheads. AP, animal pole; D, dorsal; Vg, vegetal pole; nt, notochord; pm, presomitic mesoderm.

wnt11 Expression Domain Is Expanded in Dorsalized and Reduced in Ventralized Gastrulae

If low Bmp activity specifies extension movements and underlying mediolateral cell polarity, the question arises as to how these instructions are carried out. We reasoned that Bmp might regulate dorsal convergence and extension movements by limiting activity of the *wnt11/slb* gene previously shown to be essential for extension movements but not cell-fate specification (Heisenberg *et al.,* 2000). In *slb* mutants, similar to *din* mutants (Fig. 3A), anteroposterior elongation of labeled cell groups is impaired (Heisenberg *et al.,* 2000). In WT late gastrulae, the blastopore region, paraxial head mesoderm, and dorsoanterior neuroectoderm express *wnt11* (Figs. 8B and 8F; Heisenberg *et al.,* 2000; Makita *et al.,* 1998). We found that the anterior mesoderm and ectodermal domains, as well as the blastopore domain (Figs. 8A and 8E), of *wnt11* expression were expanded in *sbn* mutant embryos. Conversely, *wnt11* expression was downregulated in ventralized *din* (Figs. 8C and 8G) and dramatically downregulated in *boz din* mutants (Figs. 8D and 8H). We conclude that high Bmp activity negatively regulates *wnt11* expression, thereby restricting the dorsal convergence and extension domain of the zebrafish gastrula. Injections of *wnt11* RNA, at doses that suppressed the *slb* phenotype in progeny of $slb^{-/-}$ parents (uninjected were 100% *slb*, $n = 83$; *slb* RNA injected were

66% WT, 34% *slb*, $n = 50$), did not rescue axis extension of *din* mutant embryos, as determined by phenotype of embryos at 9.5 and 24 hpf (uninjected were 49% WT, 51% *din*, $n = 47$; *slb* RNA injected were 48% WT, 52% *din*, $n = 163$). Therefore, while *wnt11* function is essential for extension movements (Heisenberg *et al.*, 2000), its overexpression in embryos with dorsally expanded Bmp activity is not sufficient for normal convergent extension.

wnt5a Expression in Paraxial Mesoderm Is Downregulated in Ventralized Mutants

A role for *wnt5a* in convergent extension was first implicated by its overexpression in frog embryos, which disrupt morphogenetic movements (Moon *et al.*, 1993; Torres *et al.*, 1996), in a manner independent of the canonical Wnt signaling pathway (Wallingford *et al.*, 2001). Further, studies of both mouse and zebrafish *wnt5a* mutants indicate that the gene is critical for axis extension and tail formation (Rauch *et al.*, 1997; Yamaguchi *et al.*, 1999). We tested a possible relationship between *wnt5a* and Bmp activity by examining *wnt5a* expression in WT, dorsalized, and ventralized embryos at the end of the gastrula period (10 hpf). In WT embryos, expression is strongest in the trunk and tailbud mesendoderm, extending slightly anteriorly on the dorsal side into the presomitic mesoderm, a region where cells are mediolaterally elongated and intercalation occurs (Fig. 8J). This is consistent with the expression patterns previously reported for the tailbud and somitic mesoderm at early segmentation stages (Rauch *et al.*, 1997). While the presomitic *wnt5a* expression domain is clearly present in dorsalized embryos (Fig. 8I), it is absent in ventralized *din* mutant embryos (Fig. 8K). Therefore, in addition to limiting *wnt11* expression as described above, elevated Bmp activity downregulates *wnt5a* expression in a region where normally mediolateral intercalation of cells contributes to axis extension.

DISCUSSION

Bmp Activity Gradient Specifies Three Morphogenetic CE Domains

In the vertebrate gastrula, the ventral to dorsal Bmp morphogen gradient is thought to specify cell fates (Dosch *et al.*, 1997; Harland and Gerhart, 1997; Nguyen *et al.*, 1998; Wilson *et al.*, 1997). Here, by measuring embryonic tissues and movements of cell populations *in vivo*, we demonstrate that the Bmp activity gradient plays an instructive role in regulating the spatial distribution of convergence and extension movements in zebrafish gastrulae. We propose that high ventral levels of Bmp activity inhibit convergence and extension, but promote vegetalward migration of the mesoderm, specifying the NCEZ. Laterally, decreasing Bmp levels specify increasing convergence and extension movements. Whether within this domain the transition between "slow" and "fast" convergence occurs gradually or at a specific point spatially and/or temporally is unclear. In dorsal regions, at low Bmp activity, substantial extension occurs with only limited convergence (Fig. 9A). In support of this model, the quantification of movements of labeled cell populations of WT gastrulae revealed the presence of three morphogenetic domains within the Bmp activity gradient characterized by different speed and magnitude of convergence and extension movements. Furthermore, the three morphogenetic domains are reduced or expanded in ventralized *din* and dorsalized *sbn* mutants. Our work indicates that the Bmp activity gradient establishes distinct morphogenetic domains of convergence and extension movements along the dorsoventral axis of the zebrafish gastrula, providing an important framework for analysis of specific cell behaviors in these regions.

The Role of CE Movements in Generating Embryonic Morphology

Morphometric and *in vivo* movement analyses of WT and mutant embryos demonstrate that the overall gastrula shape and elongation of the nascent embryonic axis are critically dependent on the degree of convergence and extension movements, as well as their confinement to the dorsolateral regions of the embryo. Therefore, suppressed extension and convergence movements in lateral and dorsal regions of *din* mutants account for a shortened axis and an overall rounder gastrula shape (Figs. 2 and 9F). Supporting the notion that this phenotype is a function of compromised CE movements and not an effect of altered dorsoventral patterning on other morphogenetic processes, a similar phenotype has been documented in *trilobite* (*tri*) and *knypek* (*kny*) mutants, in which CE movements but not dorsoventral patterning are defective (Sepich *et al.*, 2000; Topczewski *et al.*, 2001). The importance of dorsally restricting CE movements becomes clear from analysis of *sbn* mutants, where the expansion of the dorsal domain of strong extension and moderate convergence contributes to the elongated gastrula morphology and embryonic axis relative to WT (Figs. 2 and 5). The ectopic ventrolateral extension and convergence movements may be the major force that blocks axis elongation around the yolk cell during segmentation (Kimmel, 1989), stalling the head rudiment at the animal pole and causing premature tail eversion at the vegetal pole (Figs. 2 and 9H).

Through Inhibition of CE and Promotion of Vegetally Directed Migration of the Mesoderm, High Bmp Activity Promotes Formation of Posterior Structures

Genetic evidence in mouse and frog, and experimental embryology in frog, suggests that the ventral to dorsal gradient of Bmp activity can influence the anterior–posterior organization of vertebrate embryos (Gerhart *et al.*,

1989). Ventralized mutants exhibit an enlarged tail and smaller head and trunk (Fisher *et al.*, 1997; Hammerschmidt *et al.*, 1996; Schulte-Merker *et al.*, 1997). Moreover, in *boz din* mutants, the dramatic expansion of Bmp activity leads to an accumulation of mesodermal cells in the enlarged tailbud and a complete absence of head and trunk (Gonzalez *et al.*, 2000; Figs. 4 and 9G). Here, we show by cell movement and fate mapping experiments that WT cells residing at the highest levels of Bmp activity (in NCEZ) do not converge dorsally, nor engage in extension movements, but rather migrate to the tailbud (Fig. 4). The progressive dorsal expansion of the NCEZ in ventralized *din* and highly ventralized *boz din* mutants provides an explanation for the formation of an enlarged tailbud in these mutants and reduced (*din;* Fig. 9B) or missing (*boz din;* Fig. 9C) head and trunk. Conversely, the ventral cells of *sbn* mutants do not migrate efficiently to the tailbud and engage in ectopic extension movements assuming more anterior somitic fates (Mullins *et al.*, 1996; Fig. 5). Furthermore, we show by transplantation that overexpression of CA-BRIA can cell-autonomously promote posterior migration and inhibit extension (Fig. 4). Hence, in vertebrate embryos, the highest levels of Bmp activity specify posterior fates, in part by inhibition of convergence and extension movements, and in part by promoting vegetalward migration of the mesoderm cells.

Low Bmp Activity Specifies Dorsally Biased Cell Intercalation

Our results identify mediolateral cell polarity as a behavior through which Bmp activity can impact CE. Groups of labeled cells in the *sbn* ventral margin form elongated arrays during gastrulation (Fig. 5). At the end of the gastrula period and early segmentation, these mutant cells mediolaterally align and elongate (Fig. 6) and intercalate slowly toward the dorsal midline (Fig. 7). Together, these observations indicate that, at low Bmp activity, the dorsal domain of strong extension and limited dorsal convergence driven by mediolateral intercalation has expanded around the circumference of the *sbn* embryo. We hypothesize that these cells are pulled by the intercalation of dorsolateral cells, generating a force that constricts the embryo, causing it to elongate the animal–vegetal axis and narrow mediolaterally (Fig. 2). Eventually, the constriction displaces the yolk toward the animal pole while the vegetal cells squeeze off the yolk, forming a tail that begins curling up, creating the characteristic dorsalized "snailshell" morphology (Mullins *et al.*, 1996). Details of specific cell behaviors employed by WT and *sbn* cells in terms of protrusive activity remain to be elucidated.

A Bmp Activity Gradient Coordinates Cell Fate Specification with CE

It has been proposed that Bmp is a morphogen, specifying different cell types in the mesodermal and ectodermal layers of vertebrate gastrula at distinct activity levels (Dosch *et al.*, 1997; Wilson *et al.*, 1997; Nikaido *et al.*, 1997). Our work revealed that the same Bmp activity gradient also regulates convergent extension movements during zebrafish gastrulation. An important question arises: What is the relationship between Bmp-directed cell fate and movement behaviors? Two simple models can be proposed, though variations are possible. In one, gastrulation cell movement behaviors established at a specific Bmp activity are a consequence of specific cell fate. In other words, Bmp acts in a linear manner through a single pathway, influencing expression of cell fate specification genes, which in turn would impact the activity of genes regulating cell movement behaviors. Consequently, in this model, Bmp activity thresholds specifying cell fates and movement behaviors are the same. In the second model, Bmp specifies cell movement behaviors independently from specifying cell fate. Bmp activity thresholds defining specific cell movement behaviors could then differ from thresholds defining specific cell fates.

We argue against cell movements being merely a consequence of specific cell fate based on several lines of evidence. First, the timing of cell fate specification only follows the onset of differences in cell movements during gastrulation. Work investigating cell specification within the neuroectoderm suggests that a cell responding to Bmp signaling integrates its exposure over time and that activation of genes involved in refinement of dorsoventral pattern into specific cell fates occurs late in gastrulation (Barth *et al.*, 1999). We observed that abnormalities in the shape of mutant gastrulae and the movements of cell populations are manifested by midgastrulation (Figs. 2 and 5), suggesting that cell movements are altered before specific cell fates are defined. Second, we found similarities in cell morphologies at the same level of Bmp activity in ectoderm and mesoderm at the late gastrula stage, implying that a similar morphogenetic program operates in both germ layers, despite disparate fates (Fig. 6).

If Bmp acts to affect cell movements in parallel to cell fate specification, then it should regulate a class of genes that are involved in cell movement but not cell fate specification. One candidate is the gene *wnt11/slb* (Heisenberg *et al.*, 2000; Tada and Smith, 2000). We found that the *wnt11/slb* expression domain is enlarged in dorsalized *sbn* mutants, correlating with ectopic convergence and extension movements. Conversely, in *din* mutants, expression is reduced and is reduced or absent in highly ventralized *boz din* mutants. Therefore, in WT embryos, Bmp activity may restrict cell behaviors that drive CE movements dorsally, by limiting *wnt11/slb* expression (Fig. 8). However, we demonstrate that *wnt11* expression is not sufficient to drive extension movements in ventralized embryos and is therefore likely not the only gene required for extension movements that is regulated by Bmp activity. Accordingly, we

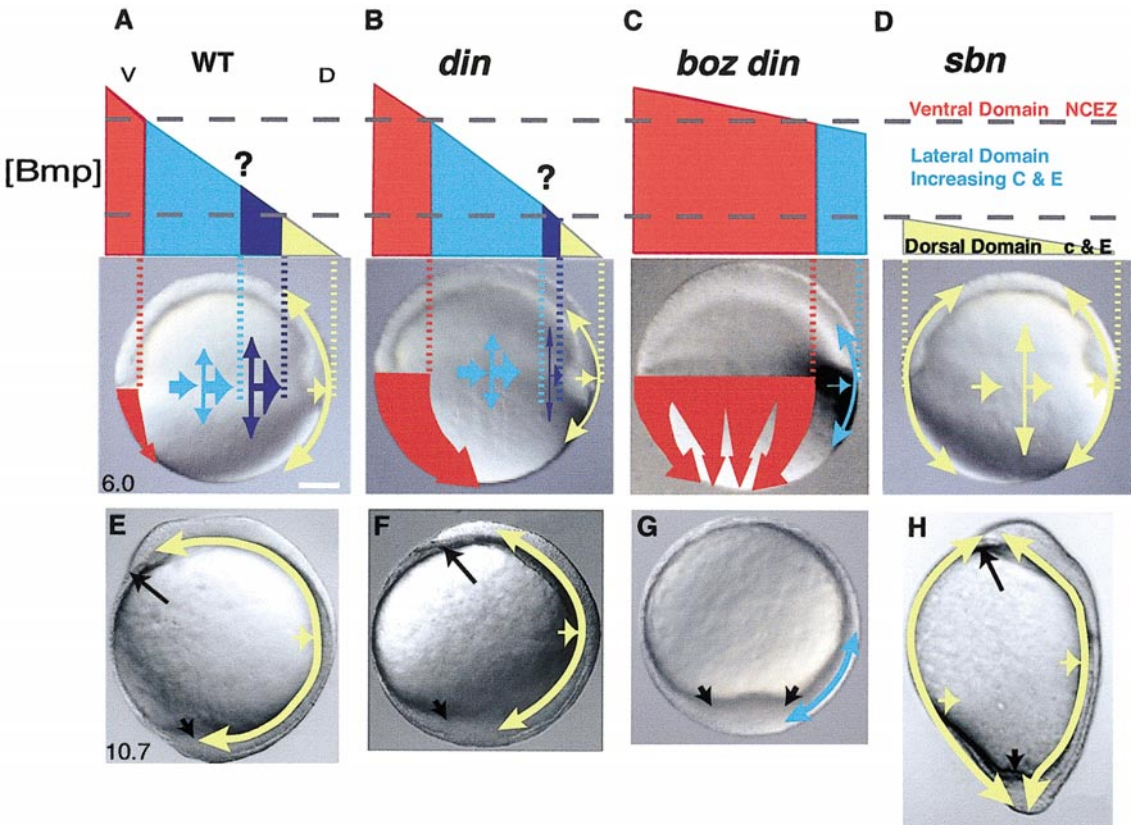

FIG. 9. Model: Bmp activity gradient specifies convergence and extension movement domains. Thresholds of Bmp activity (dashed gray lines) specify three CE movement domains. (A) In WT, high ventral Bmp levels specify NCEZ (red). An intermediate level of Bmp activity specifies increasing convergence and extension, where cells initially converge and extend slowly (light blue) and then at a faster speed (dark blue). The transition point from slow to fast convergence is unclear (question mark; light blue to dark blue). In contrast, low levels of Bmp activity specify generous extension with limited convergence (yellow). In DV patterning mutants, these movement domains are altered according to changes in the Bmp activity gradient. In ventralized (B) *din* and (C) *boz din*, the NCEZ is enlarged with increased Bmp activity, while convergence and extension are reduced in lateral regions. The domain of increasing lateral convergence and dorsal convergent extension are also reduced in *din* and may be absent in *boz din* double mutants. (D) However, in *sbn*, low levels of Bmp activity around the circumference of the embryo promote strong extension and low convergence in all regions. The distribution and degree of these morphogenetic movements shapes the early segmentation embryo. (E) In WT, NCEZ cells move to the tailbud, while lateral movements sweep cells toward the dorsal domain, where CE drives the elongation of the axis (yellow). (F, G) In *din* and *boz din*, due to reduced lateral convergence and extension, fewer cells contribute to the anterior structures, while expanded NCEZ creates enlarged tailbud, increasing posterior structures at the expense of head and trunk. (H) In *sbn*, circumferential CE movements elongate the An-Vg axis, and may eventually impair the extension of the embryonic axis. Anterior end of head (long arrow); posterior end of axis, tailbud (short arrow). Scale bar, 100 μm.

show that expression of *ppt* (*wnt5a*) in paraxial mesoderm is missing in ventralized mutant embryos (Fig. 8K). Notably, downregulation of *wnt5a* expression in paraxial mesoderm of *din* mutants is not simply a consequence of altered cell fates, as reduced somites expressing *myoD* do form in these mutants (Fig. 3D).

Overall, this work strongly advocates the idea that the Bmp activity gradient plays an instructive role in establishing distinct morphogenetic domains of convergence and extension movements along the dorsoventral axis of zebrafish gastrulae. Furthermore, it provides the basis for an intriguing hypothesis, that by regulating activities of signaling pathway(s) required for specific morphogenetic movements, like Wnt11/Wnt5a, possibly in parallel to cell fate specification, the Bmp activity gradient coordinates cell fate specification with the morphogenetic process of convergent extension. Recent work investigating the role of FGF signaling in vertebrate gastrulation and neurulation supports this hypothesis by also highlighting the extraordinary interconnectedness of patterning and morphogenesis (Ciruna and Rossant, 2001; Mathis *et al.*, 2001).

ACKNOWLEDGMENTS

We thank B. Appel, B. Hogan, C. Henry, M. Gannon, F. Marlow, and J. Jessen for critical reading of the manuscript, and members of our lab for discussions and comments. We are indebted to C.-P. Heisenberg for his advice on *slb in situ* hybridization. We acknowledge B. Heher and J. Clanton for excellent fish care. cDNA clones were provided by S. Amacher, M. Hammerschmidt, H. Takeda, R. Toyama, N. Ueno, and P. Blader, and fish strains were from M. Mullins and M. Halpern. This work is supported by NIH Grant GM55101 (to L.S.K.), who is a Pew Scholar.

REFERENCES

Barth, K. A., Kishimoto, Y., Rohr, K. B., Seydler, C., Schulte-Merker, S., and Wilson, S. W. (1999). Bmp activity establishes a gradient of positional information throughout the entire neural plate. *Development* **126,** 4977–4987.

Ciruna, B., and Rossant, J. (2001). FGF signaling regulates mesoderm cell fate specification and morphogenetic movement at the primitive streak. *Dev. Cell* **1,** 37–49.

Concha, M. L., and Adams, R. J. (1998). Oriented cell divisions and cellular morphogenesis in the zebrafish gastrula and neurula: A time-lapse analysis. *Development* **125,** 983–994.

Cooper, M. S., D'Amico, L. A., and Henry, C. A. (1999). Confocal microscopic analysis of morphogenetic movements. *Methods Cell Biol.* **59,** 179–204.

Djiane, A., Riou, J., Umbhauer, M., Boucaut, J., and Shi, D. (2000). Role of frizzled 7 in the regulation of convergent extension movements during gastrulation in *Xenopus laevis. Development* **127,** 3091–3100.

Dosch, R., Gawantka, V., Delius, H., Blumenstock, C., and Niehrs, C. (1997). Bmp-4 acts as a morphogen in dorsoventral mesoderm patterning in *Xenopus. Development* **124,** 2325–2334.

Elul, T., and Keller, R. (2000). Monopolar protrusive activity: A new morphogenic cell behavior in the neural plate dependent on vertical interactions with the mesoderm in *Xenopus. Dev. Biol.* **224,** 3–19.

Fekany, K., Yamanaka, Y., Leung, T., Sirotkin, H. I., Topczewski, J., Gates, M. A., Hibi, M., Renucci, A., Stemple, D., Radbill, A., Schier, A. F., Driever, W., Hirano, T., Talbot, W. S., and Solnica-Krezel, L. (1999). The zebrafish *bozozok* locus encodes Dharma, a homeodomain protein essential for induction of gastrula organizer and dorsoanterior embryonic structures. *Development* **126,** 1427–1438.

Fisher, S., Amacher, S. L., and Halpern, M. E. (1997). Loss of cerebum function ventralizes the zebrafish embryo. *Development* **124,** 1301–1311.

Gerhart, J., Doniach, T., and Steward, R. (1991). Organizing the *Xenopus* organizer. In "Gastrulation. Movements, Patterns, and Molecules" (R. Keller, W. H. Clark, Jr., and F. Griffin, Eds.), pp. 57–78. Plenum Press, New York and London.

Gonzalez, E., Fekany-Lee, K., Carmany-Rampey, A., Erter, C., Topczewski, J., Wright, C. V. E., and Solnica-Krezel, L. (2000). Head and trunk development in zebrafish requires inhibition of Bmp signaling by bozozok and chordino. *Genes Dev.* **14,** 3087–3092.

Graff, J. M., Thies, R. S., Song, J. J., Celeste, A. J., and Melton, D. A. (1994). Studies with a *Xenopus* BMP receptor suggest that ventral mesoderm-inducing signals override dorsal signal *in vivo. Cell* **79,** 169–179.

Hammerschmidt, M., Pelegri, F., Mullins, M. C., Kane, D. A., van Eeden, F. J. M., Granato, M., Brand, M., Furutani-Seiki, M., Hafter, P., Heisenberg, C.-P., Jiang, R. N., Odenthal, J., Warga, R. M., and Nusslein-Volhard, C. (1996). *dino* and *mercedes*, two genes regulating dorsal development in the zebrafish embryo. *Development* **123,** 95–102.

Harland, R., and Gerhart, J. (1997). Formation and function of Spemann's organizer. *Annu. Rev. Cell Dev. Biol.* **13,** 611–667.

Heisenberg, C. P., Tada, M., Rauch, G. J., Saude, L., Concha, M. L., Geisler, R., Stemple, D. L., Smith, J. C. F., and Wilson, S. W. (2000). Silberblick/Wnt11 mediates convergent extension movements during zebrafish gastrulation. *Nature* **405,** 76–81.

Hild, M., Dick, A., Rauch, G. J., Meier, A., Bouwmeester, T., Haffter, P., and Hammerschmidt, M. (1999). The smad5 mutation somitabun blocks Bmp2b signaling during early dorsoventral patterning of the zebrafish embryo. *Development* **126,** 2149–2159.

Jones, C. M., Lyons, K. M., Lapan, P. M., Wright, C. V. E., and Hogan, B. L. M. (1992). DVR-4 (Bone Morphogenetic Protein-4) as a posterior-ventralizing factor in *Xenopus* mesoderm induction. *Development* **115,** 639–647.

Jones, C. M., and Smith, J. C. (1998). Establishment of a BMP-4 morphogen gradient by long-range inhibition. *Dev. Biol.* **194,** 12–17.

Kane, D. A., and Warga, R. M. (1994). Domains of movement in the zebrafish gastrula. *Semin. Dev. Biol.* **5,** 101–109.

Kanki, J. P., and Ho, R. K. (1997). The development of the posterior body in zebrafish. *Development* **124,** 881–893.

Keller, R., and Danilchik, M. (1988). Regional expression, pattern and timing of convergence and extension during gastrulation of *Xenopus laevis. Development* **103,** 193–209.

Keller, R., Davidson, L., Edlund, A., Elul, T., Ezin, M., Shook, D., and Skoglund, P. (2000). Mechanisms of convergence and extension by cell intercalation. *Philos. Trans. R. Soc. Lond. B Biol. Sci.* **355,** 897–922.

Keller, R., Shih, J., and Domingo, C. (1992). The patterning and functioning of protrusive activity during convergence and extension of the Xenopus organiser. *Dev. Suppl.*, 81–91.

Keller, R., Shih, J., Wilson, P., and Sater, A. (1991). Pattern and function of cell motility and cell interactions during convergence and extension in *Xenopus.* In "Cell–Cell Interactions in Early Development: The 49th Symposium of the Society for Developmental Biology" (J. Gerhart, Ed.), Vol. xviii, pp. 31–62. Wiley-Liss, New York.

Keller, R. E., Danilchik, M., Gimlich, R., and Shih, J. (1985). The function and mechanism of convergent extension during gastrulation of *Xenopus laevis. J. Embryol. Exp. Morphol.* **89,** 185–209.

Kimmel, C. B. (1989). Genetics and early development of zebrafish [Review]. *Trends Genet.* **5,** 283–288.

Kimmel, C. B., Warga, R. M., and Kane, D. A. (1994). Cell cycles and clonal strings during formation of the zebrafish central nervous system. *Development* **120,** 265–276.

Kimmel, C. B., Warga, R. M., and Schilling, W. S. (1990). Origin and organization of the zebrafish fate map. *Development* **108,** 581–594.

Kimmel, C. B., Ballard, W. W., Kimmel, S. R., Ullmann, B., and Schilling, T. F. (1995). Stages of embryonic development of the zebrafish. *Dev. Dyn.* **203,** 253–310.

Koos, D. S., and Ho, R. K. (1998). The *nieuwkoid* gene characterizes and mediates a Nieuwkoop-center-like activity in zebrafish. *Curr. Biol.* **8,** 1199–1206.

Kozlowski, D. J., Murakami, T., Ho, R. K., and Weinberg, E. S. (1997). Regional cell movement and tissue patterning in the zebrafish embryo revealed by fate mapping with caged fluorescein. *Biochem. Cell Biol.* **75,** 551–562.

Makita, R., Mizuno, T., Kuroiwa, A., Koshida, S., and Takeda, H. (1998). Zebrafish wnt11: Pattern and regulation of the expression by the yolk cell and no tail activity. *Mech. Dev.* **71,** 165–176.

Mathis, L., Kulesa, P. M., and Fraser, S. E. (2001). FGF receptor signaling is required to maintain neural progenitors during Hensen's node progression. *Nat. Cell Biol.* **3,** 559–566.

Moon, R. T., Campbell, R. M., Christian, J. L., McGrew, L. L., Shih, J., and Fraser, S. (1993). Xwnt-5A: A maternal Wnt that affects morphogenetic movements after overexpression in embryos of *Xenopus laevis*. *Development* **119,** 91–111.

Mullins, M. C., Hammerschmidt, M., Kane, D. A., Odenthal, J., Brand, M., van Eeden, F. J. M., Furutani-Seiki, M., Granato, M., Hafter, P., Heisenberg, C.-P., Jiang, Y.-J., Kelsh, R. N., and Nusslein-Volhard, C. (1996). Genes establishing dorsoventral pattern formation in the zebrafish embryo: The ventral specifying genes. *Development* **123,** 81–93.

Nguyen, V. H., Schmid, B., Trout, J., Connors, S. A., Ekker, M., and Mullins, M. C. (1998). Ventral and lateral regions of the zebrafish gastrula, including the neural crest progenitors, are established by a *bmp2b/swirl* pathway of genes. *Dev. Biol.* **199,** 93–110.

Nikaido, M., Tada, M., Saji, T., and Ueno, N. (1997). Conservation of BMP signaling in zebrafish mesoderm patterning. *Mech. Dev.* **61,** 75–88.

Nikaido, M., Tada, M., Takeda, H., Kuroiwa, A., and Ueno, N. (1999). In vivo analysis using variants of zebrafish BMPR-1A: Range of action and involvement of Bmp in ectoderm patterning. *Development* **126,** 181–190.

Peifer, M., and Polakis, P. (2000). Wnt signaling in oncogenesis and embryogenesis: A look outside the nucleus. *Science* **287,** 1606–1609.

Piccolo, S., Agius, E., Leyns, L., Bhattacharyya, S., Grunz, H., Bouwmeester, T., and De Robertis, E. M. (1999). The head inducer Cerberus is a multifunctional antagonist of Nodal, BMP and Wnt signals. *Nature* **397,** 707–710.

Piccolo, S., Sasai, Y., Lu, B., and De Robertis, E. (1996). Dorsoventral patterning in Xenopus: Inhibition of ventral signals by direct binding of chordin to BMP-4. *Cell* **86,** 589–598.

Rauch, G. J., Hammerschmidt, M., Blader, P., Schauerte, H. E., Strahle, U., Ingham, P. W., McMahon, A. P., and Haffter, P. (1997). Wnt5 is required for tail formation in the zebrafish embryo. *Cold Spring Harbor Symp. Quant. Biol.* **62,** 227–234.

Schoenwolf, G. C., and Smith, J. L. (2000). Gastrulation and early mesodermal patterning in vertebrates. *Methods Mol. Biol.* **135,** 113–125.

Schulte-Merker, S., Lee, K. J., McMahon, A. P., and Hammerschmidt, M. (1997). The zebrafish organizer requires *chordino*. *Nature* **387,** 862–863.

Sepich, D. S., Myers, D. C., Short, R., Topczewski, J., Marlow, F., and Solnica-Krezel, L. (2000). Role of the zebrafish trilobite locus in gastrulation movements of convergence and extension. *Genesis* **27,** 159–173.

Shih, J., and Keller, R. (1994). Gastrulation in *Xenopus laevis:* Involution–a current view. *Sem. Dev. Biol.* **5,** 85–90.

Sokol, S. Y. (1996). Analysis of Dishevelled signalling pathways during *Xenopus* development. *Curr. Biol.* **6,** 1456–1467.

Solnica-Krezel, L. (1999). Pattern formation in Zebrafsih: Fruitful liasons between embryology and genetics. *Curr. Top. Dev. Biol.* **41,** 1–35.

Solnica-Krezel, L., Schier, A. F., and Driever, W. (1994). Efficient recovery of ENU-induced mutations from the zebrafish germline. *Genetics* **136,** 1401–1420.

Tada, M., and Smith, J. C. (2000). Xwnt11 is a target of *Xenopus* Brachyury: Regulation of gastrulation movements via Dishevelled, but not through the canonical Wnt pathway. *Development* **127,** 2227–2238.

Topczewski, J., Sepich, D. S., Myers, D. C., Walker, C., Amores, A., Lee, Z., Hammerschmidt, M., Postlethwait, J., and Solnica-Krezel, L. (2001). The zebrafish glypican Knypek controls cell polarity during gastrulation movements of convergent extension. *Dev. Cell* **1,** 251–264.

Torres, M. A., Yang-Snyder, J. A., Purcell, S. M., DeMarais, A. A., McGrew, L. L., and Moon, R. T. (1996). Activities of the Wnt-1 class of secreted signaling factors are antagonized by the Wnt-5A class and by a dominant negative cadherin in early *Xenopus* development. *J. Cell Biol.* **133,** 1123–1137.

Trinkaus, J. P. (1998). Gradient in convergent cell movement during *Fundulus* gastrulation. *J. Exp. Zool.* **281,** 328–335.

Trinkaus, J. P., Trinkaus, M., and Fink, R. (1992). On the convergent cell movements of gastrulation in *Fundulus*. *J. Exp. Zool.* **261,** 40–61.

Wallingford, J. B., Rowning, B. A., Vogeli, K. M., Rothbacher, U., Fraser, S. E., and Harland, R. M. (2000). Dishevelled controls cell polarity during *Xenopus* gastrulation. *Nature* **405,** 81–85.

Wallingford, J. B., Vogeli, K. M., and Harland, R. M. (2001). Regulation of convergent extension in *Xenopus* by Wnt5a and Frizzled-8 is independent of the canonical Wnt pathway. *Int. J. Dev. Biol.* **45,** 225–227.

Warga, R. M., and Kimmel, C. B. (1990). Cell movements during epiboly and gastrulation in zebrafish. *Development* **108,** 569–580.

Westerfield, M. (1996). "The Zebrafish Book." Univ. of Oregon Press, Eugene, OR.

Wilson, P. A., Lagna, G., Suzuki, A., and Hemmati-Brivanlou, A. (1997). Concentration-dependent patterning of the *Xenopus* ectoderm by BMP4 and its signal transducer Smad1. *Development* **124,** 3177–3184.

Yamaguchi, T., Bradley, A., McMahon, A. P., and Jones, S. (1999). A *Wnt5a* pathway underlies outgrowth of multiple structures in the vertebrate embryo. *Development* **126,** 1211–1223.

Received for publication May 9, 2001
Revised September 18, 2001
Accepted October 25, 2001
Published online January 22, 2002